Sensors and Actuators B 137 (2009) 586–591

Contents lists available at ScienceDirect

Sensors and Actuators B: Chemical

journal homepage: www.elsevier.com/locate/snb

Low cost, portable, fast multiparameter data acquisition system for organic transistor odour sensors

A. Das[a,*], R. Dost[a], T.H. Richardson[a], M. Grell[a], D.C. Wedge[b], D.B. Kell[b], J.J. Morrison[c], M.L. Turner[c]

[a] Physics and Astronomy, University of Sheffield, Hicks Building, Hounsfield Road, Sheffield S3 7RH, UK
[b] Manchester Interdisciplinary Biocentre, 131 Princess Street, Manchester M1 7DN, UK
[c] School of Chemistry, The University of Manchester, Oxford Road, Manchester M13 9PL, UK

ARTICLE INFO

Article history:
Received 17 September 2008
Received in revised form
21 November 2008
Accepted 4 January 2009
Available online 19 January 2009

Keywords:
Organic field effect transistor
Amorphous polymer
Multiparameter sensor
Fast and automated data acquisition
Chemical sensor

ABSTRACT

We demonstrate a cost-effective but fast multiparameter data acquisition system for odour sensors based on low threshold organic field effect transistors (OFETs) with an amorphous methoxy-derivative of poly(triaryl amine) (PTA-OMe) as semiconductor. The system applies a simple algorithm to measure OFET saturated transfer characteristics with a tailored operational amplifier circuit that is interfaced to a laptop that controls the circuit and analyses data with bespoke software. Despite the semiconductor's low charge carrier mobility $\mu \sim 5 \times 10^{-5}$ Vs/cm^2, the system returns multiparameter OFET data: OFET source–drain current I_{SD} in both the 'on' and 'off' state, carrier mobility μ, and threshold (V_T), in real time (resolution <1 s). The system is tested by exposing the OFET to a series of alcohol odours at different concentrations. Sensor response is quick, and follows a distinct trend IPA > PrOH > EtOH > MeOH.

1. Introduction

Organic semiconductors are now well established as cheap electronic materials in many applications, e.g. OLED, organic field effect transistor (OFET), RF-tag [1,2]. One application of organic semiconductors that is currently emerging is their use in sensor systems, sometimes known as 'electronic noses' when sensors are read electrically. The versatility of organic chemistry allows the attachment of specific functional groups for highly sensitive sensors, the celebrated example being the work of Swager and co-author on the (optical) sensing of the explosive, TNT, with a functionalised poly(*p*-phenylene ethynylene) [3]. The most generic electronically read, organic semiconductor-based sensor concept is the 'chemiresistor', where the electric resistance of a material is monitored under odour exposure, cf. e.g. the review by Bai and Shi [4]. Recently, sensors based on organic field effect transistors (OFETs) have received increasing interest [5,6]. In an OFET, the application of a gate voltage V_G above a given threshold, V_T, leads to charge carrier accumulation, turning the transistor 'on'. The OFET's source–drain current, I_{SD}, in the 'on' state may be several orders-of-magnitude larger than in the 'off' state with no gate voltage applied, when the OFET behaves similar to a chemiresistor. Most OFET-based sensor research has used this mode of operation, where the OFET acts as 'amplified' chemiresistor [7–9]. In principle, however, OFET sensors allow a more sophisticated mode of operation, where the transistor undergoes a full characterisation rather than simple monitoring of I_{SD}. The most common 'full characterisation' of an OFET comprises the recording of a saturated transfer characteristic, that is I_{SD} vs. V_G, with source–drain voltage (V_{SD}) kept larger or equal to V_G. A saturated transfer characteristic allows separate extraction of carrier mobility, μ, threshold V_T, and off-current, or on/off ratio. Recording saturated transfer characteristics therefore allows access to a 'multiparameter' data set, which is a rich resource for the assessment of odour response. Torsi et al. [10] have first reported on OFET sensors under multiparameter characterisation, showing enhanced selectivity thanks to the simultaneous extraction of several parameters. However, saturated transfer characteristics are typically recorded with laboratory-based electrometers or semiconductor parameter analysers, which are expensive, immobile due to their weight, dependent on mains electricity, and often work slower than the action of many poisons. For a practical multiparameter sensor system, we require a low-cost, battery powered mobile unit that returns multiparameter data in 'real time', i.e. faster than the action of a poison. Nevertheless, the unit needs to record reliable data even for OFETs with low I_{SD}, because organic semiconductors tailored for specific recognition may display lower carrier mobility

* Corresponding author.
E-mail address: a.das@sheffield.ac.uk (A. Das).

0925-4005/$ – see front matter.
doi:10.1016/j.snb.2009.01.006

than 'good' OFET materials such as pentacene, or regioregular poly(thiophene)s, which were developed for high mobility, but not sensitivity.

We have recently reported on an OFET characterisation circuit based on battery-powered operational amplifiers (OpAmps), and an experimental algorithm, that allows the recording of OFET saturated transfer characteristics by the trimming of potentiometers (trim potis) alone, which we call 'gain method' [11]. The potential of this system for multiparameter sensing has been confirmed by us when we applied it to find sensitive response of an OFET to NO_2 odour [12]. However, we still needed to collect data by manually trimming potis, and plot results in appropriate form, to gain multiparameter sensor data.

Here, we describe an automated version of above sensor readout scheme. In the OpAmp characterisation circuit, we replaced the manual trim potis with digital potentiometer ICs, and interfaced the circuit to a laptop, which powers the OpAmps from its battery, runs bespoke software to trim digital potentiometers, records saturated transfer characteristics, performs automated data analysis, and displays OFET parameters on screen in real time. To demonstrate the system's workings even with a low-mobility organic semiconductor, we run a generic test on an OFET using an amorphous semiconductor, a methoxy-substituted poly(triaryl amine) (PTA-OMe), under exposure to a series of alcohols.

2. Experimental

2.1. Organic semiconductor and OFET preparation

As active layer for the OFET used here, we prepared the amorphous organic semiconductor, 4-methoxy-2-methy polytriarylamine (PTA-OMe), shown in Fig. 2 as inset, by modification of the palladium catalysed polymerisation of 4-methoxy-2-methylaniline with 4,4′-dibromobiphenyl as described in detail elsewhere [13]. Transistors were fabricated using OTS-treated anodised Al 'fingers' as high-capacitance gate insulator ($C_i \approx 640$ nF/cm^2), spin casting of the semiconducting polymer from 10 g/L solution in toluene, and evaporation of Au top contacts, giving channel width and length 2 mm and 10 μm, respectively. Details of OFET preparation are given in our previous reports [11,12].

2.2. Data acquisition and processing

OFETs are characterised by the same circuit and experimental algorithm as described previously [11]. However, the algorithm is now run automatically rather than manually. The circuit is shown in Fig. 1a. Automatic control is facilitated by using digital potentiometer ICs as pulldown (R_p) and gain (R_g) resistors. Besides trimming of potis, running the characterisation algorithm requires the application of voltage steps, V_S, to the OFET's source and recording the voltage output, V_{OUT}. For automated control of all these functions, the circuit is realised on a printed circuit board (PCB), and interfaced to a laptop via a USB-based ECON data acquisition system from Data Translation.

The ECON data acquisition module uses 3 digital output channels to control the digipots: a chip select, a clock and a data channel. The gain poti is located on an analog devices AD5235 chip, which accepts 24-bit serial instructions: a 4-bit command, 4-bit address and 16 bits of data. The pulldown resistor is located on an analog devices AD7376 chip which accepts a 7-bit data-word. These two chips are 'daisy-chained' together via a serial data output channel on the AD7376 chip. Each instruction to the PCB therefore comprises 31 bits, the first 24 bits passing to the gain chip and the last 7 bits controlling the pulldown poti. The gain chip has a maximum resistance of 25 kΩ, split into 1024 steps. The pulldown poti (R_p) has a maximum resistance of 1 MΩ and 128 steps. In addition to digital outputs, the data acquisition module has a fixed +5 V output, 2 analog output channels and 16 analog input channels. One of the analog output channels provides the input signal, V_S, to the OFET. The other channel produces a constant voltage of −10 V. This voltage and the fixed +5 V output are used to supply the OpAmps.

Prior to transistor characterisation an offset correction is performed by trimming the OpAmp with a wiper (R_{Trim}) of 25 kΩ. Trim adjustment is reset before each experiment to get rid of any temporal drift from the baseline. A bespoke computer program, written in Visual Basic, controls all further input and output operations of the data acquisition module. The computer program allows setting the duty cycle frequency, V_S range and V_S step-size. Here, we have chosen V_S between 1.5 and 2.5 V in 0.2 V intervals, and a 30 Hz symmetric duty cycle for real-time characterisation.

First, choice of pulldown, R_p, has to be matched to a particular OFET, depending on its channel 'on' resistance, R_{SD}. R_p shall be approximately 1000 times smaller than R_{SD}, so that in turn, the required gain, G, of the OpAmp voltage amplifier circuit is ≈1000. At this gain, the present OpAmp (OP637) works well with minimum noise at optimised gain band width. To set R_p, the program chooses a square wave with $V_S = 2.0$ V as input, and dials a gain of $G \approx 1000$ by setting gain poti, R_g, to 2 kΩ, so that $G = R_f/R_g + 1 \approx 1000$. R_p is then set via a series of estimates. Each estimate is derived from the previous estimate by assuming that V_{OUT} is proportional to R_p, and iterations are continued until V_{OUT} is as close as possible to V_S. It takes approximately 1 s to adjust R_p, and this does not have to be repeated during characterisation.

For characterisation, V_S is set to its chosen initial level (here, $V_S = 1.5$ V), and V_{OUT} is read. Then, gain is adjusted via trimming R_g until $V_{OUT} = V_S$ for the positive half-cycles via a series of estimates in the same manner as for R_p. R_g, R_p, and V_{OFF} (=V_{OUT} for negative half-cycle) are recorded, V_S is stepped up to the next level, and the algorithm is repeated until the final V_S level is reached (here, $V_S = 2.5$ V).

For analysis, we use Eq. (1) [11], that describes the relationship between G (calculated via $G = R_f/R_g + 1$), the charge carrier mobility μ, and the threshold voltage V_T:

$$\frac{V_S}{G} = \frac{W}{2L} R_p \mu C_i (V_S - V_T)^2 \quad (1)$$

where W is the OFET channel width, L is the channel length and C_i is the capacitance per unit area of the insulating area.

Eq (1) suggests a plot of $(V_S/G)^{1/2}$ vs. V_S, resulting in a straight line with its intercept with the abscissa equal to V_T, and its slope proportional to μ. The software performs a 'virtual' plot using 'least squares' linear regression on the values of $(V_S/G)^{1/2}$. Before regression, the values of V_S are adjusted by subtracting the corresponding $|V_{OFF}|$ values, so that only field effect currents are taken into account. The quality of fit is assessed with the Pearson correlation coefficient, R^2. At a 30 Hz duty cycle, the entire procedure takes less than 1 s.

The laptop window displays information that is updated in real time (Fig. 1). This includes an oscilloscope showing V_S, V_{OUT}, R_p, G, channel on resistance, R_{SD}, V_T and μ. Users may optionally view an additional window that displays graphs of OFET on current, I_{SD} (calculated via $I_{SD} = V_S/(GR_p)$), V_T and μ values, and OFET off current I_{OFF}, calculated from V_{OFF}, as a function of time. As data are obtained they are also written to comma-separated value (csv) files. Recorded data include G, V_{OFF}, μ, V_T and Pearson coefficient. Screenshots of the oscilloscope may also be automatically saved to file.

2.3. Alcohol odour delivery

To test the OFET and characterisation system, the OFET was placed into a sealed chamber and connected to the PCB via feedthroughs. Odours of the alcohols methanol (MeOH), ethanol

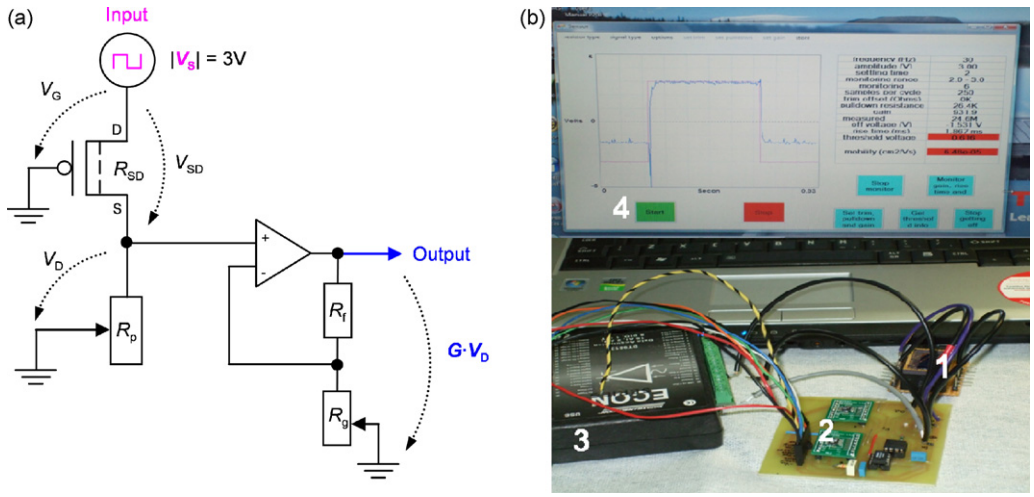

Fig. 1. (a) Scheme of voltage divider/voltage amplifier for 'gain method' OFET characterisation. $R_f = 2\,M\Omega$, R_p, R_g are digital potentiometers. (b) Laptop-supported OFET characterisation setup: (1) OFET in standard socket (to be placed in exposure chamber); (2) the circuit from a) with computer-controlled digital potentiometers (digipots) for R_p and R_g; (3) data acquisition interface; (4) laptop display and user panel, showing V_S (purple), and V_{OUT} (blue). (For interpretation of the references to colour in this figure legend, the reader is referred to the web version of the article.)

(EtOH), 1-propanol (PrOH), and 2-propanol (IPA) were created by bubbling N_2 at a flow rate of 25 standard cubic centimeter minute (sccm), resulting in the highest concentration (C_{max}) of the respective alcohol, to be calibrated later. Flow rate is controlled by Tylan FC-260 mass flow controller. C_{max} is diluted by mixing with pure N_2 carrier gas in different ratios via another Tylan mass flow controller which in the present investigation adds 25 sccm of N_2 for half dilution of C_{max}, then 50 sccm for 1/3 of C_{max} and similarly for 1/4 and 1/5 of C_{max}.

The concentration delivered to the OFET sample is important for correlating to sensor response and depends on a number of factors, including partial pressure, temperature, flow rate, and bubbler configuration [14]. Hence a calibration was carried out for all alcohols based on weight loss after bubbling with a flow rate of 25 sccm of N_2 for 3 to 4 min at a fixed temperature (22 °C). Weight change of a vapour before and after N_2 bubbling is averaged out per minute and then converted to molar concentration by dividing by its corresponding molecular weight (MW). Fig. 2 displays a plot of molar loss per minute of all alcohols used in the present study against $P_o/(P - P_o)$ where P is atmospheric pressure and P_o the partial pressure for each alcohol at that temperature. P_o data are taken from [15] and listed in Table 1. The observed linearity in Fig. 2 for all alcohols is clear indication that carrier gas generates and takes

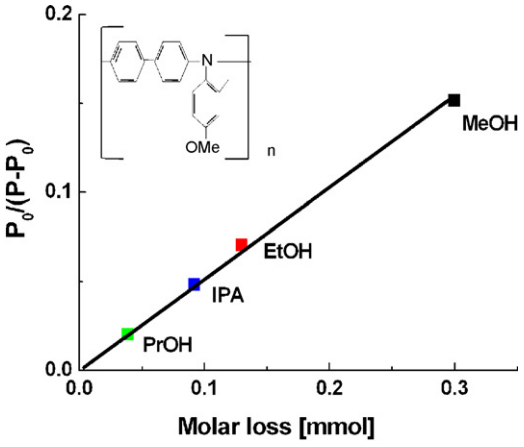

Fig. 2. Calibration curve for vapour delivery system. Inset is molecular formula of PTA-OMe.

away vapour from the bubbler in proportion to the partial pressure of that vapour. In order to compare the response of the sensor to different alcohol vapours at the same flow conditions, weight loss per minute of individual alcohols is transformed to ppm (parts per million) with respect to 25 sccm of N_2 flow (1.115 mmol) and thus calculated C_{max} are given in Table 1, also.

3. Results and discussion

Fig. 3 shows the multiparameter response of the PTA-OMe transistor when successively exposed to different concentrations of MeOH, EtOH, PrOH, and IPA, as monitored by the system described above. After each exposure, sensors are left to recover under pure N_2 purge. All sensor parameters for MeOH, EtOH, PrOH do recover at room temperature within 5 min, which indicates a rather weak binding between PTA-OMe and these alcohols. Recovery after IPA exposure takes somewhat longer, exposure cycles have therefore been kept shorter, as well (~1 min; for other odours exposure time varied from 2 to 3 min, as indicated by the width of the shaded bands in Fig. 3). Note the mobility of the amorphous PTA-OMe is rather low, in the order 10^{-5} cm^2/Vs, but the system still delivers low noise measurement in real-time. We also note that generally, we need to expose our sensor to rather high alcohol odour concentrations, in the range 10^3 to 10^6 ppm, to get a clear response. However, this is not surprising, as the semiconductor employed here is a generic material, which was not engineered to have particularly strong or specific interactions with the analytes. Instead, it was chosen to provide a test run for the automated multiparameter data acquisition system under challenging conditions (low mobility).

Fig. 3 displays various multiparameter responses recorded as a matter of different alcohol vapour exposures to PTA-OMe OFET. The first data set for each odour, I_{SD} in the OFET 'on' state, would be the only set of data available to a conventional 'amplified chemiresistor' type OFET sensor without multiparameter characterisation. A reduction in 'on' current, and mobility, under exposure is clearly observed for all alcohols.

To quantify the sensor response to the different alcohols, Fig. 4 shows the change in source–drain current for different alcohol odours and concentrations, all after 1 min exposure, calculated from the data shown in Fig. 3. It is immediately obvious that the sensor response per ppm IPA is significantly stronger than for the other alcohols. Since both $\Delta I/I$ vs. ppm, and $\Delta\mu/\mu$ vs. ppm plots are approximately linear for lower concentrations, the slopes

Table 1
Summary of molecular parameters, and normalised sensor response for the odours studied here.

Name	P_o (mmHg)	M_w (g/mol)	C_{max} (ppm)	$(\Delta I/I)$/ppm ($\times 10^{-6}$)	$(\Delta\mu/\mu)$/ppm ($\times 10^{-6}$)	$\Delta(D)$	β_{KT}
MeOH	108	32	270,000	2.4 ± 0.1	2.4 ± 0.1	1.7	0.62
EtOH	50	46	117,000	2.7 ± 0.2	5.2 ± 0.2	1.69	0.77
PrOH	17	60	35,000	5.9 ± 0.3	15.4 ± 0.3	1.68	0.79
IPA	35	60	82,500	16.5 ± 0.4	24.6 ± 0.3	1.66	0.92

P_o: partial pressures (from [15]); M_w: molecular weights; $\Delta(D)$: molecular dipole moment (from [16]); β_{KT}: Kamlet–Taft basicity parameter (from [19]).

$(\Delta I/I)$/ppm or $(\Delta\mu/\mu)$/ppm at lower ppm may be taken as a quantitative measure of sensor response. In turn, if it is known which alcohol the OFET is exposed to, Fig. 4 can be used as a calibration that allows reading odour concentration from an observed sensor response. At higher odour concentrations, response may approach saturation. Table 1 lists $(\Delta I/I)$/ppm calculated from Fig. 4a, and $(\Delta\mu/\mu)$/ppm from Fig. 4b, together with a few other molecular characteristics taken from the literature.

According to Table 1, the strength of the OFET's response to a given partial pressure of alcohol odour ranks in the order of IPA > PrOH > EtOH > MeOH, both for normalised saturated drain current (I_{SD}) response and normalised mobility response. In terms of normalised I_{SD} response, PrOH, EtOH, MeOH are in the same order of magnitude, but IPA gives an order of magnitude stronger response than the other alcohols. While I_{SD}(on) currents would be the only data accessible to a conventional 'amplified chemiresistor' sensor characterisation, the real-time, multiparameter setup introduced here gives us more detailed information on the sensor response. Charge carrier mobility, μ, is rather low to begin with, yet still drops significantly under exposure, e.g. down to less than 1/3 of its pre-exposure value under C_{max} MeOH. The strength of mobility response, $(\Delta\mu/\mu)$/ppm, ranks in the same way as $(\Delta I/I)$/ppm, but spans the observed range more evenly.

The observed ranking cannot be explained by the molecular dipole moment (Δ), because Δ is almost identical for all alcohols, largely controlled by the defining –OH group. However, it is most likely that an interaction between PTA-OMe and the –OH group determines the sensor response. As p-type semiconductor, PTA-OMe carries positive charges on its backbone during OFET operation, and we propose these will interact with the lone electron pair of oxygen in the alcohol group, with the semiconductor acting as Lewis acid, and the alcohol as Lewis base. The Lewis base strength of an alcohol is quantified by the Kamlet–Taft (K–T) basicity parameter, β_{KT} [17,18]. β_{KT} values for the alcohols used here are

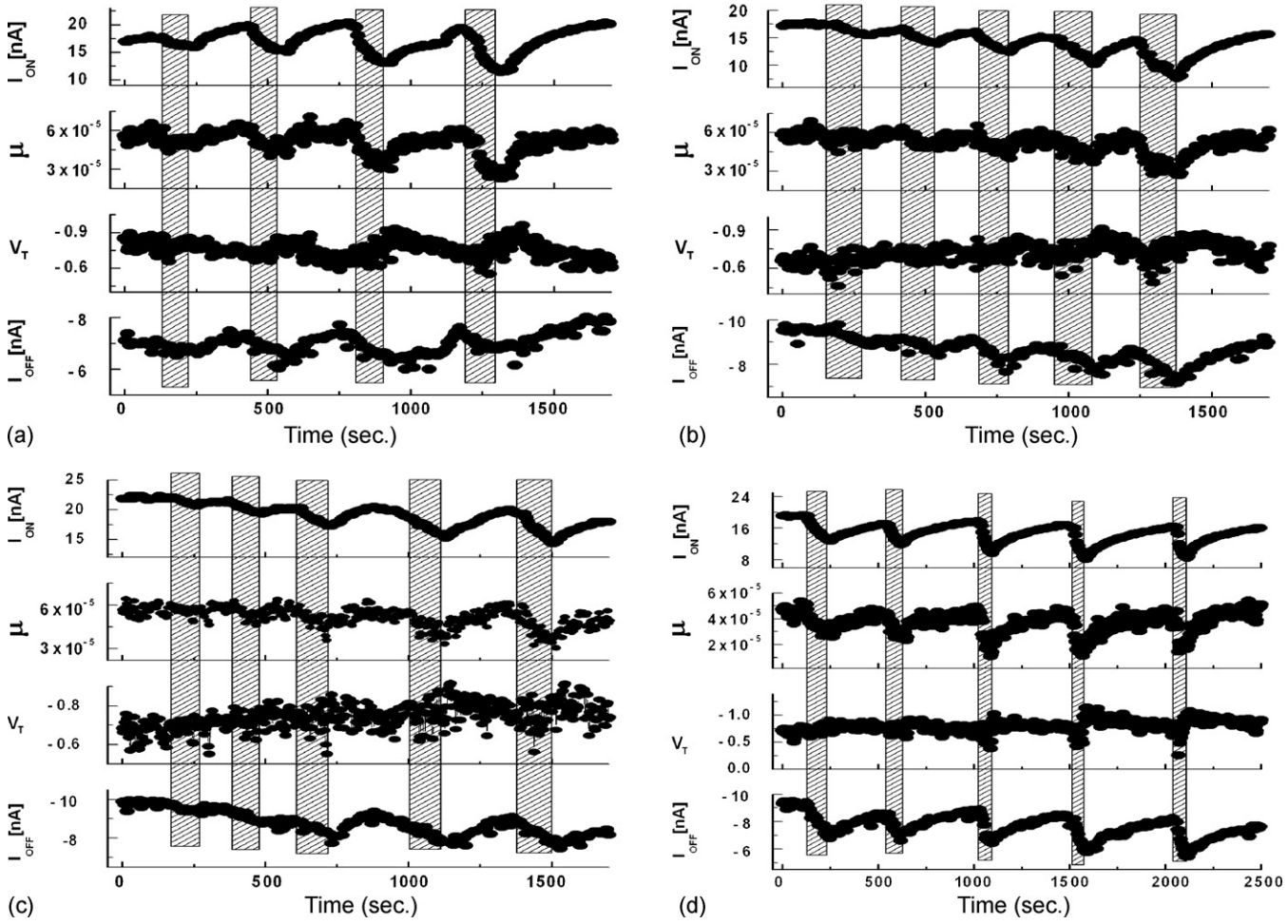

Fig. 3. Multiparameter response of PTA-OMe OFET for exposure/recovery cycles under different alcohols: (a) MeOH, (b) EtOH, (c) PrOH, and (d) IPA. Shown are the OFET source–drain current I_{SD} in the 'on' state (V_S = +2.5 V), carrier mobility (in cm^2/Vs), threshold voltage, OFET source–drain current in the 'off' state (V_S = −2.5 V). Shaded areas indicate exposure, beginning with the most dilute ($1/5C_{max}$) for all alcohols except MeOH ($1/4C_{max}$), and progressively increasing. Exposure cycles are 2–3 min in length, recovery at least 2 min, apart from IPA exposure cycles, which are kept shorter (1 min), and the OFET is left to recover for longer after IPA exposure.

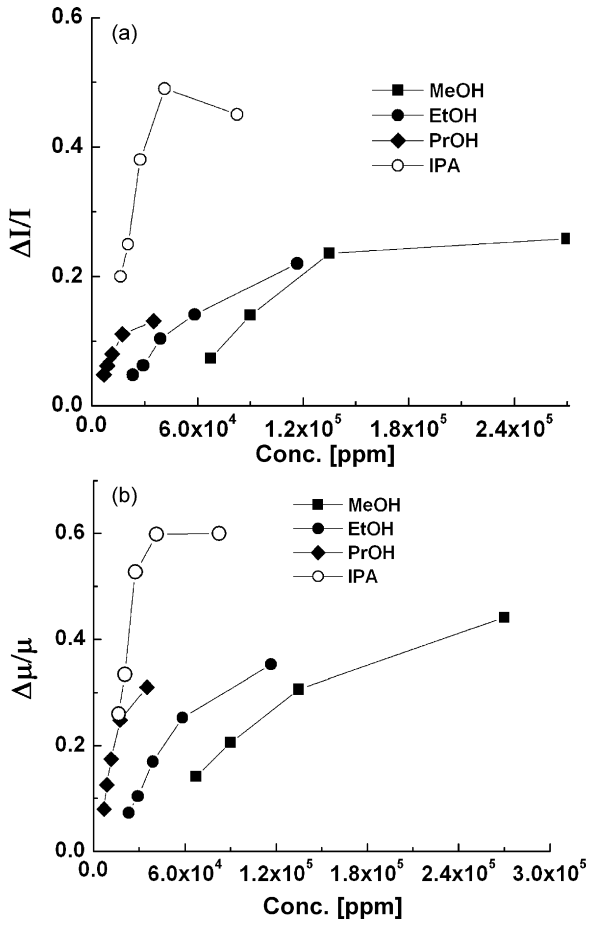

Fig. 4. Normalised reduction in OFET: (a) on-current at $V_S = 2.5$ V, and (b) mobility obtained after 1 min under exposure to different alcohol odours and concentrations, where $\Delta I/I = [I(1\,\text{min}) - I(\text{before})]/I(\text{before})$, and similarly for $\Delta\mu/\mu$.

also listed in Table 1, and we find they rank in the same order as normalised sensor response (Fig. 5), which supports our hypothesis of odour/semiconductor interaction.

Threshold, V_T, also responds to odour exposure, albeit not quite as clearly. Apart from IPA, response is weak and the V_T scale has to be expanded, which leads to a rather noisy appearance, making V_T a less useful sensor parameter than μ in the current example. However, V_T response under exposure reveals a surprise, which is best observed on the IPA data: threshold clearly decreases in the modulus value (i.e. approaches zero), under exposure. Then a rise also is observed (Fig. 3) under the same exposure. Interestingly, such shift in V_T does not reflect directly in I_{SD} measurements (Fig. 3). All else being equal, a decrease in threshold would lead to an *increase* in the on-current [12], contrary to the observed decrease. However, all else is not equal: the big decrease in μ overwhelms the variation in V_T, resulting in overall smaller on-current. Still, the observations of modulation in V_T as well as opposing trends in μ and V_T are a piece of information accessible only to multiparameter characterisation, and would be lost under simple on-current monitoring. We have previously observed a strong reduction of threshold, down to zero, when a similar OFET was exposed to the oxidising odour, NO_2 [12], due to oxidative doping of the p-type semiconductor. However, alcohols are not oxidising, and we will see in the discussion of off-current that there is no evidence of doping by the odours here. Instead, the weaker reduction as well as the rise in V_T observed here may be due to the cumulative effects of shielding of built-in fields in the transistor [20], contacts and trapping of charges [1], which are known to contribute to threshold by the polar alcohol.

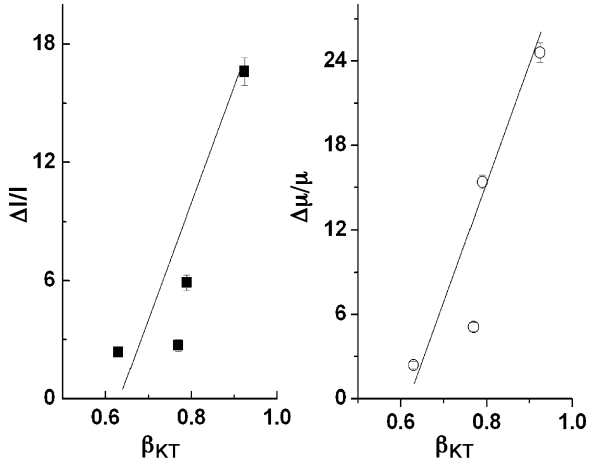

Fig. 5. This figure shows plot of normalised responses from alcohol exposures for both mobility and on-current against *K*–*T* parameters. Linear fits are to guide the eye only.

Finally, Fig. 3 demonstrates the capability of our system to monitor another sensing parameter, the OFET's drain current in the 'off' state, I_{OFF}. In the 'off' state, conductivity is provided by the inevitable small concentration of dopants present in any organic semiconductors, and the OFET essentially acts as a simple chemiresistor. As long as 'off'-currents are not many orders-of-magnitude smaller than 'on' currents, it is easy to monitor drain currents in the 'off' state, as well as in the 'on' state, with our measurement scheme, simply by recording GV_D in the 'off' half-cycle of the V_S-drive scheme. In fact, for data analysis, our software algorithm subtracts 'off'-currents from 'on' currents before extraction of μ and V_T, to correct for any currents contributing to 'on' current that are not field effect currents. Fig. 3 shows that on this occasion, 'off'-currents are approximately 2.5 times smaller than 'on' currents. In other words, the 'on/off ratio' of our OFET is only 2.5. State-of-the-art OFETs for display applications may have on/off ratios in the order 10^5 or more [1]. The low on/off ratio is the result of the low carrier mobility in our semiconductor, and implies that PTA-OMe will not find applications in OFETs for purposes other than odour sensing. Crucially, we do observe that 'off'-currents mirror the behaviour of 'on' currents and mobility, in the sense that 'off'-current decreases under odour exposure. This clearly shows that alcohol odours do not dope the semiconductor, while oxidising odours such as NO_2 do [12], leading to a significant increase in 'off'-current, even when mobility and 'on'-current decrease. Here, in contrast, the observed reduction in 'off' current simply reflects the reduction in carrier mobility (Fig. 3).

4. Conclusions

We introduce a portable, laptop-driven multiparameter data collection system for OFET-based odour sensors, and test it under challenging conditions: we use a low mobility organic semiconductor (PTA-OMe) OFET, $\mu \approx 5 \times 10^{-5}$ Vs/cm^2, and expose it to alcohol odours, with which the semiconductor does not strongly interact. Nevertheless, we succeed in recording multiparameter sensor data in real time. Multiparameter data are a far richer source of information than simple 'on'-current monitoring of an OFET, and reveal non-obvious features of the weak interaction between odours and organic semiconductor. We believe that wider application of the proposed data acquisition scheme to OFET sensors will allow for a deeper understanding of odour/semiconductor interactions, deliver improved guidelines for the design of odour-specific materials, and eventually, will enable more sensitive and specific sensor systems.

References

[1] H. Sirringhaus, Device physics of solution-processed organic field-effect transistors, Adv. Mater. 17 (2005) 2411.
[2] A. Dodabalapur, Organic and polymer transistors for electronics, Mater. Today 9 (2006) 24.
[3] J.-S. Yang, T.M. Swager, Porous shape persistent fluorescent polymer films: an approach to TNT sensory materials, J. Am. Chem. Soc. 120 (1998) 5321.
[4] H. Bai, G. Shi, Gas sensors based on conducting polymers, Sensors 7 (2007) 267.
[5] L. Torsi, G.M. Farinola, F. Marinelli, M.C. Tanese, O.H. Omar, L. Valli, F. Babudri, F. Palmisano, P.G. Zambonin, F. Naso, A sensitivity-enhanced field-effect chiral sensor, Nat. Mater. 7 (2008) 412.
[6] L. Torsi, M.C. Tanese, N. Cioffi, M.C. Gallazzi, L. Sabbatini, P.G. Zambonin, Alkoxy-substituted polyterthiophene thin-film-transistors as alcohol sensors, Sens. Actuators B 98 (2004) 204.
[7] F. Liao, C. Chen, V. Subramanian, Organic TFTs as gas sensors for electronic nose applications, Sens. Actuators B 107 (2005) 849.
[8] L. Wang, D. Fine, A. Dodabalapur, Nanoscale chemical sensor based on organic thin film transistors, Appl. Phys. Lett. 85 (2004) 6386.
[9] L. Torsi, M.C. Tanese, N. Cioffi, M.C. Gallazzi, L. Sabbatini, P.G. Zambonin, G. Raos, S.V. Meille, M.M. Giangregorio, Side-chain role in chemically sensing conducting polymer field-effect transistors, J. Phys. Chem. B 107 (2003) 7589.
[10] L. Torsi, A. Dodalabapur, L. Sabbatini, P.G. Zambonin, Multi-parameter gas sensors based on organic thin-film-transistors, Sens. Actuators B 67 (2000) 312.
[11] R. Dost, A. Das, M. Grell, A novel characterization scheme for organic field-effect transistors, J. Phys. D: Appl. Phys. 40 (2007) 3563.
[12] A. Das, R. Dost, T.H. Richardson, M. Grell, J.J. Morrison, M.L. Turner, A nitrogen dioxide sensor based on an organic transistor, Adv. Mater. 19 (2007) 4018.
[13] I.-W. Shen, M.C. McCairn, J.J. Morrison, M.L. Turner, Synthesis of polytriarylamines via microwave-assisted palladium, Macromol. Rapid Commun. 28 (2007) 449.
[14] Y.S. Kim, S.-C. Ha, H. Yang, Y.T. Kim, Gas sensor measurement system capable of sampling volatile organic compounds (VOCs) in wide concentration range, Sens. Actuators B 122 (2007) 211.
[15] http://www.s-ohe.com.
[16] D.R. Lide (Ed.), CRC Handbook of Chemistry and Physics, CRC Press, Boca Raton, FL, 2002 http://en.wikipedia.org/.
[17] M.J. Kamlet, R.W. Taft, Solvatochromic comparison method, J. Am. Chem. Soc. 98 (1976) 377.
[18] M.J. Kamlet, J.-L.M. Abboud, M.H. Abraham, R.W. Taft, Linear solvation energy relationships. 1. Beta-scale of solvent hydrogen-bond acceptor (β) basicities, J. Org. Chem. 48 (1983) 2877.
[19] M. Khodaei, A.A. Jamali, Kinetic study of the reaction of 2,2′-bipyridyl chromium peroxide with alcohols, J. Sci. I. R. Iran 11 (2000) 105.
[20] C. Huang, H.E. Katz, J.E. West, Solution-processed organic field-effect transistors and unipolar inverters using self-assembled interface dipoles on gate dielectrics, Langmuir 23 (2007) 13223.

Biographies

Arindam Das is a research associate in the department of physics and astronomy, University of Sheffield. He received his PhD from the Indian Institute of Technology, Madras in 1999. He joined as a post-doctoral fellow at the National Taiwan University, CCMS in 2000 and then moved with Alexander von Humboldt fellowship to TU Chemnitz, Germany in 2001. During 2003–2006, he worked as a research associate in the Cardiff University, Nanophysics group with Dr. Emyr Macdonald on the SPM & GIXRD applications to polymer films. His research interests revolved around surface sciences, ion beam modification and semiconducting polymers. His current focus is to develop low cost OFET sensor for chemical odours.

René Dost graduated in 2004 as Dipl-Phys at the Technical University of Dresden, Germany, after obtaining his BSc (Hons) at the University of Northumbria, Newcastle (2002). He then returned to Great Britain and received his PhD in physics on the development of an organic sensor readout scheme from the University of Sheffield in 2008. René Dost has since been working as postdoctoral research associate at the same university with Dr. Martin Grell. His research interests include OFET and OFET-based sensor characterisation, SAMFETs, and nanometer organic electronics.

Tim Richardson received his BSc degree from University of Durham (UK) in 1985 and his doctorate from the University of Oxford (UK) in 1989. He is currently a reader in Nano-science in the department of physics & astronomy at the University of Sheffield (UK). His interests are focused on the physical properties of Langmuir–Blodgett films, principally their use as vapour-sensing materials. He is a fellow of the Institute of Physics and a fellow of the Royal Society of Chemistry.

Martin Grell is a senior lecturer in the department of physics & astronomy, University of Sheffield (UK). He received his 'Dr. rer. nat.' (PhD) in polymer physics from the Technical University, Darmstadt, Germany, in 1994. His research interest focuses in the field of organic semiconductors.

David Wedge is a post-doctoral research associate within the School of Chemistry at the University of Manchester. His interests include software development for real-time data collection and multiparameter data analysis, particularly through the use of Evolutionary Computation. He obtained a BA in chemistry from Oxford University in 1989, an MSc in software development from Huddersfield University in 2001 and a PhD in artificial intelligence from Manchester Metropolitan University in 2006.

Douglas B. Kell is a professor in the School of Chemistry, University of Manchester/UMIST and holds RSC/EPSRC chair in Bioanalytical Sciences. He received his BA (Hons) degree in 1975 from the Oxford University and DPhil in 1978. His research interests are broad, but core to them is the development of novel analytical methods for understanding complex biological systems. This often involves computational as well as 'wet' methods.

John J. Morrison received his MPhil (1994) and PhD (1997) degrees from The University of St Andrews. He then moved to do postdoctoral research on the synthesis of organic semiconductors with Prof. Andrew B. Holmes at Cambridge before returning to work in St Andrews with Prof. Russell E. Morris, Dr. Ian Shannon and Dr. Nigel P. Botting. During 2001–2002 he was an international scholar with Prof. Virgil Percec at The University of Pennsylvania. Since 2006 he has worked with Prof. Mike L. Turner in the Organic Materials Innovation Center at Manchester. Amongst wide research interests his current focus is upon the synthesis of amorphous semiconducting polymers for organic electronics applications.

M.L. Turner is a professor of materials chemistry in the Organic Materials Innovation Centre (OMIC) of the School of Chemistry, the University of Manchester. He received his PhD degree from the University of Bristol, UK. He was awarded a Royal Society University Research Fellowship in 1993 to investigate the synthesis of novel polymers at the University of Sheffield, UK. He joined the staff of the department of chemistry, University of Sheffield as a reader in 2000 and in April 2004 moved to the University of Manchester to a chair in materials chemistry and to be director of OMIC. His principal research interests concern the synthesis of novel conjugated molecules, particularly conjugated liquid crystals and conjugated polymers, and in using these novel molecules in organic electronic and electrooptical devices such as organic transistors, sensors and solar cells. This research is carried out as part of the Organic Materials for Electronics Consortium.